Optics Communications 393 (2017) 169–172

Contents lists available at ScienceDirect

Optics Communications

journal homepage: www.elsevier.com/locate/optcom

A temperature-independent fibre-optic magnetic-field sensor using thin-core fibre tailored fibre Bragg grating

Qin Tian, Zhongyao Feng*, Qiangzhou Rong*, Yun Wan, Xueguang Qiao, Manli Hu, Hangzhou Yang, Ruohui Wang, Zhihua Shao, Tingting Yang

Department of Physics, Northwest University, Taibai Beilu 229, Xi'an, Shaanxi 710069, China

ARTICLE INFO

Keywords:
Optical fibre sensor
Refractive index sensing
Magnetic fluid
Magnetic field sensing

ABSTRACT

A temperature-independent fibre-optic magnetic-field sensor is proposed and demonstrated experimentally. The device consists of a thin-core fibre (TCF) sandwiched in the upstream of a fibre Bragg grating (FBG). Because of the core-mismatch between the TCF and the single-mode fibre (SMF), the core mode is coupled to the cladding modes within the TCF cladding, and parts of them are recoupled back to the leading-in SMF by the downstream FBG. The cladding modes are sensitive to the ambient refractive index (RI), and therefore have the ability to respond to a RI change in the magnetic fluid determined by the ambient magnetic field. The intensities of the cladding-mode resonances are highly sensitive to the magnetic field change, while, in contrast, the resonance wavelengths always remain unchanged. This property can allow the sensor to act as a power-referenced reflection probe for magnetic field measurements.

1. Introduction

Magnetic-field sensors have been widely applied in many scientific and industrial applications, such as aerospace engineering, geophysical research, energy surveys, and navigation [1,2]. The magnetic field is usually detected by current-driven magnetometers that have been developed over the past several decades. However, these components have inherent drawbacks such as an inherent electromagnetic sensitivity, large size, and poor multiplexing ability. In comparison, optical fibre technology can avoid these problems and realise the detection of a magnetic field in place of electronic sensors [3–5]. Amongst the array of diverse optical devices, fibre-optic sensors have displayed excellent performances, which, in turn, have opened up a multitude of opportunities for single-point magnetic field sensing in hard-to-reach spaces, with controllable cross-sensitivities and very compact size for embedded measurements [6–8]. Because optical fibres are insensitive to a weak magnetic field, a magnetic fluid (MF), with magnetic-sensitive particles to diffuse the solution, is generally employed as a bridge for the light information and magnetic field. Once the fibre-optic refractometers are immersed in the MF, they can respond to the RI change in the MF determined by the magnetism, and thus detect the magnetic field indirectly [9]. To date, diverse fibre-optic magnetometers have been developed with improved detection sensitivity, detection range, and low-cost, including a microfibre knot resonator [10], tunable slow light device [11], dual-S-shaped integrated optic fibre [12], abrupt taper Michelson interferometer [13], and so on. Compared with these resonant components, the FBG presents a single resonance spectrum, thus conserving the spectrum occupancy and presenting a better multiplexity [14]. To improve the RI sensitivity of a FBG, a post-process operation of etching is utilised to remove the fibre cladding, and make the fibre core mode respond to the magnetic field-induced MF RI change. The magnetic field is determined through the recovery of wavelength information. However, the etched FBG presents inadequate mechanical strength and low reflectivity. Additionally, temperature cross-talk is another factor that influences precise magnetic field detection.

In this paper, a fibre-optic magnetic-field sensor is proposed and demonstrated experimentally. The fibre sensor structure consists of a thin-core fibre (TCF) sandwiched in the upstream of FBG, which is similar to the structure proposed in the paper by Yan et al., which sought to achieve a core mode for SMF coupled to the cladding of the TCF through core-mismatching between the TCF and SMF. However, in their proposed sensor, a section of TCF is inserted between the SMFs to form an in-fibre multimodal interferometer and the TCF is etched, which leads to a frail and complex structure [15]. Compared with the sensor proposed in their paper, we use the power information of the refraction spectrum of the SMF-TCF–FBG structure to achieve higher magnetic field sensitivity. In their paper, the dual parameters of the magnetic field and temperature measurement sensor use the transmission spectrum of the TCFMI structure. In our sensor, the cladding-

---

* Corresponding authors.
E-mail addresses: fengzhongyao@nwu.edu.cn (Z. Feng), qzrong2010@gmail.com (Q. Rong).

http://dx.doi.org/10.1016/j.optcom.2017.02.050
Received 22 December 2016; Received in revised form 17 February 2017; Accepted 18 February 2017

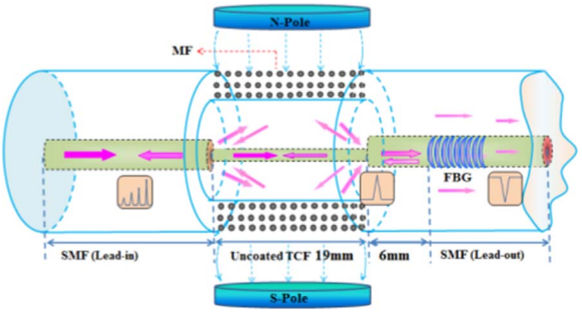

Fig. 1. Schematic diagram of the TCF-FBG-based magnetic field sensor.

mode resonances are sensitive to the power of the magnetic field-induced RI variations in the MF, but insensitive to temperature. Furthermore, the sensor has better mechanical properties than the sensors fabricated by tapering, core-offset, or cladding-etched methods [2,15,16]. Therefore, this device can act as a temperature-independent sensor through the recovery of power information.

2. Sensor design and principle

The schematic diagram of the TCF-tailored FBG (TCF-FBG) is shown in Fig. 1, in which the diameters of the core and cladding of the TCF are 4.2 μm and 80 μm, respectively. As the TCF is spliced to the SMF, and because of the core-mismatching between them, the core mode is coupled to the cladding of the TCF, resulting in the cladding mode generations propagating along the cladding of the TCF. Parts of the cladding modes are recoupled back to the leading-in SMF. Several cladding mode resonances appear on the short side of the reflection spectrum, and the core mode resonance is posted on the long side. The refraction spectrum is clearly shown in Fig. 2. In general, the backward transmission high-order cladding modes will be absorbed by the surrounding high-index materials and cannot propagate for a long distance within the fibre cladding. However, once the reflected cladding modes are recoupled into the fibre core, they can propagate over a long distance with a transmission loss as low as that of the core mode. To decrease extra power absorption, the jacket material on the TCF-FBG section is removed. It is known that normal FBG is insensitive to the RI because of its thick cladding, confining the light transmission to the core. In this device, the TCF is a key component of the sensor. The cladding modes within the TCF cladding have the ability to couple out the cladding and then become lost in the ambient medium. The intensities of the cladding modes are determined by the ambient change in RI. As the MF covers the area surrounding the sensor, the magnetic field-induced MF RI change can be detected by recovering the intensity information. Because the ambient RIs do not influence the resonance frequencies of the cladding modes, the wavelengths of the resonance spectra always remain unchanged. The temperature variations within the same range are the main cause for the TCF-FBG length change, and they slightly influence the effective index profiles of the cladding modes [16]. As a result, the spectral wavelengths present a shift with temperature, but the spectral intensities remain almost unchanged.

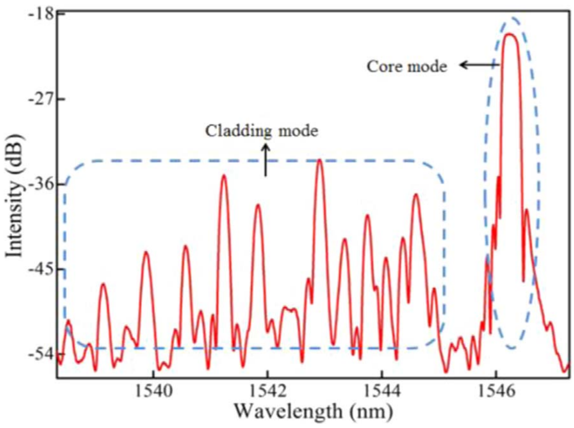

Fig. 2. Refraction spectrum of the TCF-FBG structure.

The refraction spectrum of the SMF-TCF-SMF structure shifts with the change in SRI [17], while the wavelength of the Bragg core reflection remains unaffected. Therefore, the peak power of the core reflection can be tailored by the perturbation in SRI through the invisible SMF-TCF-SMF (FBG) structure output spectrum.

3. Experiment and discussion

The RI response of the TCF-FBG is characterised as follows. To keep the sensor straight and the strain constant, two fibre holders are used to eliminate the influence of bend and stress. A 19-mm long groove is fixed on the lifting table to ensure that the sensing region is completely immersed in liquid. A series of water-glycerol solutions with different concentrations are prepared as samples (ranging from 1.3758 to 1.4249), which are calibrated by an Abbe refractometer.

For each specific liquid RI value measurement, the 19-mm long groove is filled with the RI liquid using a pipette so that the TCF-FBG structure is completely immersed in the RI liquid. After each test, the sensor is cleaned with alcohol and distilled water, and then is air-dried until the spectrum returns to its original output. Throughout the entire experiment process, the temperature environment is kept at 25 °C. The cladding-mode reflection spectrum changes with the change in the liquid RI from 1.3758 to 1.4249. A good linear response identified as a function of the SRI is plotted in Fig. 3. It is quite clear that the power changes with the increase in the liquid RI, but the wavelength remains nearly unchanged. Finally, a liquid RI sensitivity of −234.92 dBm/RIU is achieved. Compared with refractive index sensors of the same type in the 1.3375–1.4249 range [18–20], this device is more sensitive to the liquid refractive index.

The MF used in the experiment is a highly stable aqueous solution of ferromagnetic nanoparticles whose average diameter is smaller than 10 nm. The particle density of the MF is 1.18 g cm/10^3 and the scope of the saturated magnetisation is 0 mT to 20 mT. The MF RI with an original value of 1.42 decreases with the increase in the magnetic field. Because of the initial magnetisation and the saturated magnetisation of the MF, the reflective intensity of many intensity-interrogated magnetic field sensors based on magnetic fluid exhibit linear behaviours within a limited range [2,21]. To realise the TCF-FBG-based magnetometer, the structure is placed into a glass capillary tube completely filled with MF. Both sides of the structure are held in place at the two

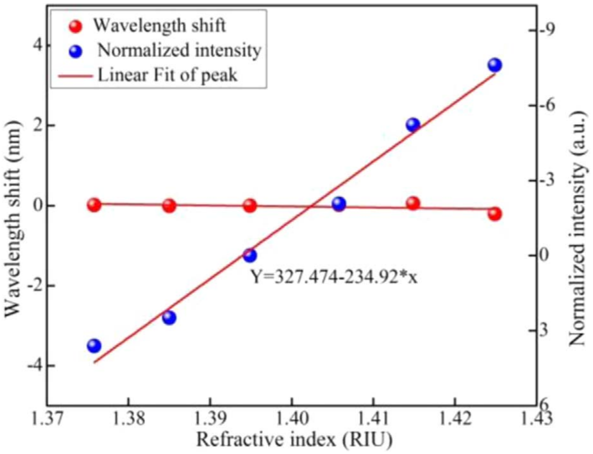

Fig. 3. Intensity and wavelength response to the SRI of the cladding mode with reflection.